

# All-order relativistic many-body calculations for the electron affinities of $\text{Ca}^-$ , $\text{Sr}^-$ , $\text{Ba}^-$ and $\text{Yb}^-$ negative ions

Euripides N. Avgoustoglou and Donald R. Beck

*Physics Department, Michigan Technological University, Houghton, Michigan 49931*

(January 27, 1997)

## Abstract

Electron affinities are evaluated for negative ions formed by the attachment of one electron to atoms with closed subshells using relativistic many-body perturbation theory. In particular, we investigate the  $\text{Ca}^-$ ,  $\text{Sr}^-$ ,  $\text{Ba}^-$ , and  $\text{Yb}^-$  ions. Starting from a model space that consists of nondegenerate valence Dirac-Hartree-Fock orbitals, we first approximate the energy of the attached electron as the lowest eigenvalue of a second-order effective Hamiltonian. Higher-order correlation corrections are calculated in the linear cluster approximation. The Breit interaction is also included in first order. Our results are in good agreement with recent experiments and show a clear improvement over the second-order Dyson equation. Comparisons with other many-body calculations are also presented.

31.15.Ar, 31.15.Md, 31.25.Eb, 32.10.Hq

Typeset using REVTeX

## I. INTRODUCTION

Over the years, negative ions have attracted an increasing interest both from the experimental and the theoretical standpoint. Especially, after the review article by Hotop and Lineberger [1] and the monograph by Massey [2], substantial developments on the experimental techniques led to highly accurate measurements, as well as new predictions, of several electron affinities providing an outstanding challenge for improved theoretical calculations. From more recent reviews [3–6], it becomes clear that substantial theoretical investigation is still necessary in order to achieve theoretical values of the same accuracy as the ones quoted by recent experiments.

In the present study, we calculate the electron affinities of systems where an electron is attached outside a closed subshell atom. Our basic motivation stems from recent measurements of the electron affinities of  $\text{Ca}^-$  [7] and  $\text{Ba}^-$  [9] based on the combination of laser photodetachment and resonance ionization spectroscopy and where accuracy of order 1% was accomplished. These systems, along with  $\text{Sr}^-$  [8], have also been the subject of considerable theoretical interest for the last ten years [11–27] and several computational techniques have been tested to overcome the sensitivity of the results due to correlation corrections.

From the perspective of many-body theory, studies have in principle been based on the solution of Dyson’s equation [10,15] where the proper self-energy is approximated in second order while higher-order correlation corrections were selectively included [18,22]. As it was shown by Dzuba *et al* [22], such an approach leads to the proper estimation of the fine-structure splitting but their calculated electron affinities were in poor agreement with experiment. A systematic inclusion of higher-order correlations, recently accomplished by Salomonson *et al* [27], led to a significant improvement in the agreement between theory and experiment for the electron affinities of  $\text{Ca}^-$  and  $\text{Sr}^-$ . These corrections were calculated nonrelativistically while the fine-structure splitting was still obtained from the second-order Dyson equation.

Our approach is based on relativistic Rayleigh-Schrödinger many-body perturbation theory (RMBPT) where correlations beyond second order are evaluated in the linear cluster approximation [28–30,37]. This method has been applied to atomic systems like the alkalis with one valence electron outside a closed shell leading to an agreement with experiment of order less than 0.1% [30,31]. However, in these systems the valence electron is bound due to the screened Coulomb field of the closed subshell ion, while in the negative ions under consideration the electron is much more weakly bound due to the polarization potential of the neutral atom. This difference leads to a more demanding study of correlation corrections in the latter case that can be at first realized by the lowest-order approximation to the valence-electron energy. In the alkalis, starting from the  $V^{N-1}$  Hartree-Fock (HF) model potential of the positively charged closed core, a fair approximation of the lowest-order energy of the valence electron can be obtained [32], creating an excellent starting point for the subsequent successful application of RMBPT. But in negative ions, starting from the  $V^N$  HF

potential of the neutral atom, all the single-particle valence orbitals are unbound leading to no physical realization of the attached electron as a single-particle valence state. In spite of that, we may assume that the wavefunction for the attached electron can be represented as a linear combination of unbound HF valence orbitals that are members of a nondegenerate model space [28,33]. This hypothesis is closely related to the formulation of the quasiparticle orbital of the attached electron from the second-order Dyson equation as a superposition of a complete basis set of HF orbitals [15]. By choosing the members of our model space to be the dominant components of this quasiparticle wavefunction, we are led to a matrix equation that involves the effective Hamiltonian  $H^{\text{eff}}$  [29]. After excluding the energy of the atomic core, the electron affinity can simply be defined as the opposite of the binding energy of the attached electron and this corresponds to the lowest eigenvalue of  $H^{\text{eff}}$ . This approach enables us to obtain a first approximation to the  $H^{\text{eff}}$  from second-order perturbation theory which is formally very similar to the self energy-matrix of the second-order Dyson equation [15] but of significantly lower dimension. At this level, the calculated electron affinities from the two methods are very close but they are essentially a factor of two different than the most recent experimental values. Our next step is to take advantage of the low dimension of our model space and to include systematically single and pair correlation corrections to all orders. Our final results improve the agreement with experiment to the level of 10% for the cases of  $\text{Ca}^-$ ,  $\text{Sr}^-$  and  $\text{Ba}^-$  and enable us to give an estimate for a possible positive electron affinity for the more complicated case of  $\text{Yb}^-$ .

## II. FORMALISM

Our method is developed using the formal similarities between the case of atoms with one valence electron, for example the alkalis, and the considered negative ions resulting from the attachment of one electron to a closed subshell atom. The system is described by the relativistic “no-pair” Hamiltonian [35] :

$$H = H_0 + V_I. \quad (2.1)$$

In second quantization, the model Hamiltonian  $H_0$  and the perturbation  $V_I$  are written respectively

$$H_0 = \sum_i \varepsilon_i a_i^\dagger a_i, \quad (2.2)$$

$$V_I = \frac{1}{2} \sum_{ijkl} g_{ijkl} a_i^\dagger a_j^\dagger a_l a_k - \sum_{ij} U_{ij} a_i^\dagger a_j, \quad (2.3)$$

where  $a^\dagger$ ,  $a$  stand for fermionic creation and annihilation operators and  $\varepsilon_i$ s are the positive eigenvalues of the one-electron Dirac equation

$$h(\mathbf{r}) \varphi_i(\mathbf{r}) = \varepsilon_i \varphi_i(\mathbf{r}), \quad (2.4)$$

$$h(\mathbf{r}) = c \boldsymbol{\alpha} \cdot \mathbf{p} + (\beta - 1)c^2 + V_{\text{nuc}}(r) + U(r). \quad (2.5)$$

If  $N$  is the number of core electrons, the negative ion is considered as a  $(N + 1)$  electron system and, following Ref. [15], we choose  $U(r)$  to be the  $V^N$  Hartree-Fock model potential of the atomic core defined as

$$U_{ij} = \int \varphi_i^\dagger(\mathbf{r}) U(r) \varphi_j(\mathbf{r}) d^3r = \sum_c (g_{icjc} - g_{iccj}), \quad (2.6)$$

with  $g_{ijkl}$  standing for the two-electron matrix element of the Coulomb interaction

$$g_{ijkl} = \int \int \frac{d^3r_1 d^3r_2}{r_{12}} \varphi_i^\dagger(\mathbf{r}_1) \varphi_j^\dagger(\mathbf{r}_2) \varphi_k(\mathbf{r}_1) \varphi_l(\mathbf{r}_2). \quad (2.7)$$

According to the index convention followed, the letters  $a, b, c, d$  correspond to core states;  $v, w$  correspond to valence states;  $m, n, r, s$  correspond to virtual states; and  $i, j, k, l$  correspond to all orbitals.

Our goal is to solve the time-independent many-body Schrödinger equation

$$H|\Psi\rangle = E|\Psi\rangle. \quad (2.8)$$

For the case of a particle outside a closed shell we have the following expression of the model space state vectors [36] :

$$|\Phi_v\rangle = a_v^\dagger |0_c\rangle, \quad (2.9)$$

where  $|0_c\rangle$  denotes the closed subshell ground state of the neutral atom.

In the studies related to atoms with one valence electron outside a closed core, there is essentially no mixing among valence states and the model space consists of only one state vector. But in negative ions the wavefunction of the attached electron is realized as a linear combination of several unbound orbitals [15]. Therefore in this case, the solution to the Schrödinger equation is obtained by acting with the wave operator  $\Omega_v$  on a linear combination of nondegenerate state vectors defined in Eq.(2.9). This approach was employed successfully in the case of a nearly degenerate model space for particle-hole systems [37,38], but as it has been shown theoretically by Lindgren [28], it can also be applied to this more general case of a nondegenerate model space.

The solution of Eq.(2.9) takes the form :

$$|\Psi\rangle = \sum_v C_v \Omega_v |\phi_v\rangle \quad (2.10)$$

and via the correlation operator  $\chi_v$  defined as

$$\Omega_v = 1 + \chi_v, \quad (2.11)$$

we transform Eq.(2.9) into an eigenvalue equation

$$\sum_v H_{v',v}^{\text{eff}} C_v = E C_{v'}, \quad (2.12)$$

where the effective Hamiltonian  $H^{\text{eff}}$  is given by

$$H_{v',v}^{\text{eff}} = \langle \Phi_{v'} | H(1 + \chi_v) | \Phi_v \rangle \quad (2.13)$$

and the equation for the correlation operator is

$$[\chi_v, H_0] | \Phi_v \rangle = V_I(1 + \chi_v) | \Phi_v \rangle - \sum_{v'} \chi_{v'} | \Phi_{v'} \rangle \langle \Phi_{v'} | V(1 + \chi_v) | \Phi_v \rangle. \quad (2.14)$$

We approximate the correlation operator up to pair excitations, i.e.

$$\chi \approx \sum_{ij} a_i^\dagger a_j \chi_j^i + \frac{1}{2} \sum_{ijkl} a_i^\dagger a_j^\dagger a_l a_k \chi_{kl}^{ij}, \quad (2.15)$$

and the correlation correction to the model space states defined in Eq.(2.9) becomes

$$\chi_v | \Phi_v \rangle = \left( \sum_{ma} \chi_a^m a_m^\dagger a_a a_v^\dagger + \sum_{m \neq v} \chi_v^m a_m^\dagger + \sum_{mna} \chi_{va}^{mn} a_m^\dagger a_n^\dagger a_a + \frac{1}{2} \sum_{mnab} \chi_{ab}^{mn} a_m^\dagger a_n^\dagger a_b a_a a_v^\dagger \right) | 0_c \rangle. \quad (2.16)$$

This approximation leads to the following system of coupled equations for the correlation coefficients:

$$(\varepsilon_a - \varepsilon_m) \chi_a^m = \mathcal{R}_a^m, \quad (2.17)$$

$$(\varepsilon_a + \varepsilon_b - \varepsilon_m - \varepsilon_n) \chi_{ab}^{mn} = \mathcal{R}_{ab}^{mn}, \quad (2.18)$$

$$(\varepsilon_v - \varepsilon_m) \chi_v^m = \mathcal{R}_v^m - \sum_{v'} \chi_{v'}^m \mathcal{R}_v^{v'}, \quad (2.19)$$

$$(\varepsilon_v + \varepsilon_a - \varepsilon_m - \varepsilon_n) \chi_{va}^{mn} = \mathcal{R}_{va}^{mn} - \sum_{v'} \chi_{v'a}^{mn} \mathcal{R}_v^{v'}, \quad (2.20)$$

where  $R_j^i$  and  $R_{kl}^{ij}$  are defined respectively

$$\mathcal{R}_j^i = \sum_{ma} \tilde{g}_{iajm} \chi_a^m - \sum_{mab} g_{abjm} \tilde{\chi}_{ab}^{im} + \sum_{mna} g_{iamn} \tilde{\chi}_{ja}^{mn}, \quad (2.21)$$

$$\begin{aligned} \mathcal{R}_{kl}^{ij} = & g_{ijkl} + \sum_{mn} g_{ijmn} \chi_{kl}^{mn} + \sum_{ab} g_{abkl} \chi_{ab}^{ij} + \sum_m g_{ijml} \chi_k^m - \sum_a g_{ajkl} \chi_a^i + \sum_{ma} \tilde{g}_{ajml} \tilde{\chi}_{ka}^{im} \\ & + \sum_m g_{jimk} \chi_l^m - \sum_a g_{ailk} \chi_a^j + \sum_{ma} \tilde{g}_{aimk} \tilde{\chi}_{la}^{jm}, \end{aligned} \quad (2.22)$$

with tilded terms including the exchange parts of the four indexed objects, for example  $\tilde{g}_{ijkl} = g_{ijkl} - g_{jilk}$ .

This formalism leads to the following expression for  $H^{\text{eff}}$  :

$$H_{v'v}^{\text{eff}} = \varepsilon_v \delta_{v'v} + \sum_{abm} g_{abvm} \tilde{\chi}_{ab}^{mv'} + \sum_{amn} g_{v'amn} \tilde{\chi}_{va}^{mn} + \sum_{ma} \tilde{g}_{v'avm} \chi_a^m. \quad (2.23)$$

In lowest order,  $\chi_j^i = 0$  and Eq.(2.23) becomes

$$H_{v'v}^{\text{eff}} = \varepsilon_v \delta_{v'v} + \sum_{abm} \frac{g_{abvm} \tilde{g}_{mv'ab}}{\varepsilon_a + \varepsilon_b - \varepsilon_{v'} - \varepsilon_m} + \sum_{amn} \frac{g_{v'amn} \tilde{g}_{mnva}}{\varepsilon_v + \varepsilon_a - \varepsilon_m - \varepsilon_n} \quad (2.24)$$

This relation reveals the nonhermitian nature of this method. Practically, this is only a formal disadvantage since there is always the option to force  $H^{\text{eff}}$  to be Hermitian [33], simply by defining

$$\bar{H}^{\text{eff}} = \frac{1}{2}[H^{\text{eff}} + (H^{\text{eff}})^\dagger] \quad (2.25)$$

However, for the cases under consideration, we found that the lowest eigenvalue of this matrix and that of Eq.(2.24) were different at the level of 1 meV which lies at the limits of the numerical accuracy of the present calculation. Therefore, we proceeded with the nonhermitian expression for  $H^{\text{eff}}$ . We would also like to mention an improved manifestedly hermitian formalism for  $H^{\text{eff}}$ , systematically presented by Lindgren [34], the realization of which lies beyond the scope of this work.

Even though our formalism is a rather straightforward generalization of the method presented in Ref. [30], its numerical realization is a much more complicated numerical task, mainly because of the slow convergence of the iteration process and the large basis sets necessary in order to improve the accuracy of the calculation. Our basis sets for single particle wavefunctions were created using the B-spline method [41], essentially in the same way as in Ref. [15], but we found that a choice of a larger cavity radius ( 60 a.u. instead of 40 ) helped convergence of the iteration process. Simple modifications of our code enabled us to test it directly against well established calculations before applying it for any new results. As a first test, we solved the second-order Dyson equation and we found agreement with the corresponding published values of Refs. [15,27]. The next test was to constrain our method

to a single member model space and derive the results for neutral Lithium presented in Ref. [30] and the corresponding third-order terms for neutral Cesium presented in Ref. [31].

In the application of the method to negative ions, special attention was given to the synthesis of the model space. Our criteria were based on the similarity between Eq.(2.24) and the matrix form of the second-order Dyson equation [15]

$$\sum_j (\varepsilon_i \delta_{ij} + \Sigma_{ij}^{(2)}) c_j = \varepsilon_0 c_i \quad (2.26)$$

where the self-energy matrix elements  $\Sigma_{ij}^{(2)}$  are defined as

$$\Sigma_{ij}^{(2)} = \sum_{abm} \frac{g_{abjm} \tilde{g}_{miab}}{\varepsilon_a + \varepsilon_b - \varepsilon_0 - \varepsilon_m} + \sum_{amn} \frac{g_{iamn} \tilde{g}_{mnja}}{\varepsilon_0 + \varepsilon_a - \varepsilon_m - \varepsilon_n} \quad (2.27)$$

and the quasiparticle orbital  $\psi_0(\mathbf{r})$  of the attached electron with angular quantum number  $k$  and binding energy  $\varepsilon_0$  is written as an expansion of *all* the Hartree-Fock orbitals with the same angular quantum number, i.e

$$\psi_0(\mathbf{r}) = \sum_i c_i \varphi_i(\mathbf{r}). \quad (2.28)$$

As it is shown in reference [15], a set of 25 states is a sufficient numerical realization of this expansion but still the solution of the second-order Eq.(2.26) is an expensive numerical task that results in relatively poor agreement with the most accurate recent experiments.

In the all-orders approach via  $H^{\text{eff}}$ , we found that a model space consisting of six valence states was sufficient for the second-order Eq.(2.24) to give a lowest eigenvalue less than 10% different than the binding energy  $\varepsilon_0$  of the quasiparticle wavefunction obtained from Eq.(2.26). From the similarity of these two equations it is obvious that these states have to be chosen to be the valence HF orbitals that dominate in the expansion (2.28). So technically, we used the second-order Dyson equation as the first step in our approximation. By raising the dimension of the model space, we found that the new mixing coefficients  $C_v$  of Eq.(2.10) were of magnitude  $< 0.1$  which was our cut off criterion similar to Ref. [42]. For example, in the case of  $\text{Ca}^-$ , our model space consists of six  $np_{1/2}$  valence states with  $n$  ranging from 4 to 9. The validity of this argument is shown in the following table where the six dominant amplitudes  $c_i$  of the  $4p_{1/2}$   $\text{Ca}^-$  quasiparticle orbital derived from Eq.(2.26) are opposed the coefficients  $C_v$  resulting from the solution of Eq.(2.12). The corresponding values agree at the level of 1% while the coefficients  $c_i$  account for 99.5% of the unit norm of the quasiparticle orbital.

$n$	$c_i$	$C_v$
4	0.385833	0.393995
5	-0.598645	-0.605019
6	-0.556163	-0.557406
7	0.345933	0.343157
8	-0.197454	-0.193125
9	-0.118553	-0.113864

In the summations over core orbitals, we included a certain number of outer shells. These defined our active core. By performing separate second-order calculations including all core orbitals, we found that the missing inner-core correlations were less than 5% of the calculated electron affinities similar to Ref. [27]. To go beyond second order, we solved iteratively Eqs.(2.17-2.20). After every iteration, the new correlation coefficients were used to calculate the new  $H^{\text{eff}}$  matrix from Eq.(2.23). The electron affinity is defined as the opposite of the lowest eigenvalue of this matrix. The solution of Eqs.(2.17-2.20) involves differences between core and valence orbitals. For the orbitals of the most outer core shell, these differences are small and lead to slow convergence of our method since they are involved as denominators in our iteration scheme. In order to speed up the iteration process certain truncations were necessary. For each angular quantum number  $k = \pm 1, \pm 2, \dots, \pm 11$  we created 40 basis states but we used 30 of them for the correlation corrections beyond second order. In addition, certain cut off criteria were also applied to the magnitude of the pair correlation coefficients. The numerical realization of this method was a very big computational task and was performed on the two Alpha Stations available in our group. After the truncations, the time for every iteration ranged from 24 hours CPU time for the case of  $\text{Ca}^-$  to 48 hours for  $\text{Ba}^-$  and  $\text{Sr}^-$  and 72 hours for  $\text{Yb}^-$ . Convergence is an important concern in problems of this type [39,40]. For the cases of  $\text{Sr}^-$ ,  $\text{Ba}^-$  and  $\text{Yb}^-$ , the large cost in computational time forced us to terminate the iteration process when the difference of the lowest eigenvalue of  $H^{\text{eff}}$  between two successive iterations was less than 0.1 meV. Usually, ten iterations were needed to achieve this level of numerical precision. But for the computationally less demanding case of  $\text{Ca}^-$ , we were able to test convergence using the criterion suggested by Nakano and Obara [40] which is based on the logarithm of the norm of the  $n$ -th-order ( $H_{\text{eff}}^{(n)}$ ) contribution to the  $H^{\text{eff}}$  matrix. This is taken as the difference between the resulting  $H^{\text{eff}}$  after  $n - 1$  and  $n$  iterations and is defined as

$$\|H_{\text{eff}}^{(n)}\| = \left[ \sum_{v'v} |(H_{\text{eff}}^{(n)})_{v'v}|^2 \right]^{1/2} \quad (2.29)$$

In Fig. 1, the logarithm of  $H_{\text{eff}}^{(n)}$  is presented up to twentieth-order of perturbation for the  $4p_{1/2}$  state of  $\text{Ca}^-$  while in Fig. 2 the corresponding convergence pattern of the electron affinity is shown. At the point where the iteration process was terminated, the value of the

logarithm of this norm was around -4.5 which corresponded to less than 0.05% change on the value of the electron affinity between successive iterations.

The Breit interaction can be introduced as a perturbation of the form

$$V_B = \frac{1}{2} \sum_{ijkl} b_{ijkl} a_i^\dagger a_j^\dagger a_l a_k, \quad (2.30)$$

where  $b_{ijkl}$  is the two-particle matrix element of instantaneous Breit operator  $b(\mathbf{r}_{12})$ ,

$$b(\mathbf{r}_{12}) = -\frac{1}{2r_{12}} [\alpha_1 \cdot \alpha_2 + \alpha_1 \cdot \hat{r}_{12} \alpha_2 \cdot \hat{r}_{12}]. \quad (2.31)$$

Using the expansion coefficients  $C_v$  from Eq.(2.12), we can estimate the lowest-order Breit correction

$$B^{(1)} = \sum_{vv'} C_v C_{v'} \langle \Phi_{v'} | V_B | \Phi_v \rangle \quad (2.32)$$

or with the help of relations (2.29) and (2.9)

$$B^{(1)} = \sum_{cvv'} C_v C_{v'} \check{b}_{cvcv'}. \quad (2.33)$$

The contribution of this correction was found at the 1% level of the calculated electron affinities from the Coulomb  $H^{\text{eff}}$ .

### III. RESULTS

The first step towards the numerical realization of our method was to solve the second-order Dyson equation (2.26). In addition to the importance of this calculation as the criterion for the formulation of our model space, we were also enabled in this way to set a common background for comparison with other many-body calculations. The resulting electron affinities from this approach are listed as  $E_{\text{Dyson}}^{(2)}$  in the second column of Table I. In the first column of this table, we denote the states for the attached electron using the valence orbital with the smallest principle quantum number of those six that form the model space. For example, the “ $4p_{1/2}$ ” state of  $\text{Ca}^-$  is essentially a superposition of  $4p_{1/2}, 5p_{1/2}, \dots, 9p_{1/2}$  valence states. In the third column of Table I, we present the electron affinities  $E^{(2)}$  calculated from the diagonalization of the second-order  $H^{\text{eff}}$  (2.24). Since the model space includes the orbitals that dominate in the expansion (2.28), these values differ less than 10% from  $E_{\text{Dyson}}^{(2)}$ . In comparison to the most recent experimental values for the cases of  $\text{Ca}^-$ ,  $\text{Sr}^-$  and  $\text{Ba}^-$  listed in the last column of this table, we see that the second-order calculations overestimate the electron affinities around 70% for  $\text{Ba}^-$  and 100% for  $\text{Ca}^-$  and  $\text{Sr}^-$  while

the agreement for the fine structure is better and at the level of 20% for  $\text{Ba}^-$  and  $\text{Ca}^-$  and 10% for  $\text{Sr}^-$ . The experimental values that have been chosen for comparison have explicitly measured the fine-structure splitting. A review of the experimental status, as well as most of the theoretical calculations, is presented in Ref. [26]. In the fourth column of Table I we present the calculated electron affinities  $E^{(pair)}$  in the pair approximation. We see that these values are consistently much closer to experiment. The inclusion of the lowest-order Breit  $B^{(1)}$  in column five reduces  $E^{(pair)}$  around 1% and their sum is listed as  $E^{(tot)}$  in column six of Table I. The negative sign of  $B^{(1)}$  is with respect to the electron affinity which, as we mentioned, is simply the opposite of the binding energy. For the case of  $\text{Ca}^-$ , the agreement is improved to the level of 10% for both  $4p_{1/2}$  and  $4p_{3/2}$  states. The same agreement is accomplished for the  $6p_{1/2}$  and  $6p_{3/2}$  states of  $\text{Ba}^-$  along with the  $5p_{1/2}$  state of  $\text{Sr}^-$ . For the  $5p_{3/2}$  state of  $\text{Sr}^-$ , our value of 36.8 meV leads to a fine-structure splitting of 11.1 meV that lies outside the experimental value of 26(8) meV given by Berkovits *et al* [8]. Our good agreement with all the other five cases in connection to the relatively big experimental error of this measurement, might pose a motivation for further experimental investigation of this system.

For the  $\text{Yb}^-$  we have a case that tests the validity of higher-order correlation corrections on the prediction of new electron affinities. As we can see from Table I, the second-order results  $E_{\text{Dyson}}^{(2)}$ , and  $E^{(2)}$  predict a positive electron affinity of 45 meV. This value is in agreement with the estimate of  $54 \pm 27$  meV from the density functional calculation of Vosko *et al* [23] and is approximately half the value of 98.5 meV from many-body nonrelativistic calculation of Gribakina *et al* [19]. In the latter case the active core included only the  $6s^2$  outer shell while in our case the active core included all five outer subshells. But after including higher-order correlation corrections the system became unbound. Because of the large amount of computational time needed in this case, we stopped our process one iteration after the system was found unbound. At that point, it was unbound at the level of 2 meV. Considering the numerical constraints that we posed in order to carry out this calculation and according to the consistency of our results for the previous experimentally well established cases, we claim that if  $\text{Yb}^-$  is bound, its electron affinity must be very close to the lowest possible observation threshold of 10 meV posed by the only experimental work in which this negative ion was detected [43].

In Table II, we present our results in comparison with other ab initio many-body calculations. Here, because of the numerical constraints, as well as the missing correlation corrections starting from triple excitations, the values for the calculated electron affinities were truncated at the level of 1 meV while for the less sensitive to correlation fine-structure splitting, one more significant figure was kept. The relativistic calculation of Johnson *et al* [15] corresponds to the solution of the second-order Dyson equation (2.26). Therefore their values can be directly compared to our  $E_{\text{Dyson}}^{(2)}$  of Table I. The small difference of 1 meV for  $\text{Ca}^-$  can be attributed to the slightly different basis sets while the differences for  $\text{Sr}^-$  and  $\text{Ba}^-$  occur because of the inclusion of an extra subshell in our active core. In the nonrel-

ativistic calculation of Gribakin *et al* [18], based also on the second-order Dyson equation, part of the valence states involved in the intermediate summations were created in the field of the atomic core with a hole in the outer shell. This difference in the model potential led to different estimation to order by order correlation effects. However the inclusion of selected third-order contributions brought their estimation to the level of the second-order relativistic Dyson equation using the Hartree-Fock model potential of the closed core. We note that this calculation does not distinguish between  $np_{1/2}$  and  $np_{3/2}$  levels and therefore only qualitatively can be compared with relativistic calculations as well as experiments. The posting of their results under the  $np_{1/2}$  columns is only a matter of presentation. A similar idea by Dzuba *et al* [22] of using virtual excited states, relativistically this time, in a core-hole potential along with a certain class of effects beyond second order gave also results close to  $E_{\text{Dyson}}^{(2)}$ .

The most critical comparison of our method is with respect to the recent work of Salomonson *et al* [27] for the cases of  $\text{Ca}^-$  and  $\text{Sr}^-$ . In their calculation, the correlation corrections beyond second order were also evaluated in a systematic way similar to ours but nonrelativistically. The relativistic corrections were included from the difference of a second-order Dyson equation performed both relativistically and nonrelativistically. Since we considered the same active core, their fine-structure splittings agrees precisely with the differences between the values  $E_{\text{Dyson}}^{(2)}$  of the  $p_{1/2,3/2}$  states listed in Table I. The good agreement between the two calculations shows that the intrinsically relativistic nature of our method in these cases compensates for the missing correlation corrections due to certain class of triple excitations that they included.

In conclusion, by performing a fully relativistic calculation we were able to achieve excellent agreement with the most accurate recent measurements for the electron affinities of  $\text{Ca}^-$ ,  $\text{Ba}^-$  and  $\text{Sr}^-$ . Our method was based on the formulation of an optimum nondegenerate model space combined with a systematic inclusion of correlation corrections beyond second order that had successfully tested for the similar but relatively simpler case of the alkalis. The consistency of our results and the good agreement with the more complete, but nonrelativistic beyond second order calculation by Salomonson *et al* [27], lead us to suggest a new measurement for the  $5p_{3/2}$  for  $\text{Sr}^-$ . For  $\text{Yb}^-$ , higher-order correlations led to a slightly unbound system but the approximations that we made to make the treatment of the system computationally manageable do not exclude the possibility of an electron affinity around 10 meV. In this case further theoretical as well as experimental investigation is necessary.

#### IV. ACKNOWLEDGEMENTS

We would like to acknowledge useful discussions with Professor W. Johnson. Furthermore, we thank the Computer Science Dept. of Michigan Technological University for providing substantial Computational Support of the work. This research was partially sup-

ported by the National Science Foundation Grant No. 93-17828.

## REFERENCES

- [1] H. Hotop and W. C. Lineberger, *J. Phys. Chem. Ref. Data* **4**, 539 (1975).
- [2] Massey, H. S. W., *Negative Ions*, 3rd ed., (Cambridge Univ. Press, London and New York, 1976).
- [3] Massey, H. S. W., *Adv. Atom. and Mol. Phys.* **15**, 1 (1979).
- [4] H. Hotop and W. C. Lineberger, *J. Phys. Chem. Ref. Data* **14**, 731 (1985).
- [5] D. R. Bates, *Adv. Atom. Mol. and Opt. Phys.* **27**, 1 (1990).
- [6] S. J. Buckman and C. W. Clark, *Rev. Mod. Phys.* **66**, 539 (1994).
- [7] V. V. Petrunin, H. H. Andersen, P. Balling, and T. Andersen, *Phys. Rev. Lett.* **76**, 744 (1996).
- [8] D. Berkovits, E. Boaretto, S. Ghelberg, O. Heber, and M. Paul, *Phys. Rev. Lett.* **75**, 414 (1995).
- [9] V. V. Petrunin, J. D. Voldstad, P. Balling, P. Kristensen, T. Andersen, and H. K. Haugen *Phys. Rev. Lett.* **75**, 1911 (1995).
- [10] L. V. Chernysheva, G. F. Gribakin, V. K. Ivanov, and M. Yu Kuchiev, *J. Phys. B* **21**, L419 (1988).
- [11] C. Froese-Fischer, J. B. Lagowski, and S. H. Vosko, *Phys. Rev. Lett.* **59**, 2263 (1987).
- [12] C. Froese-Fischer, *Phys. Rev. A* **39**, 963 (1989).
- [13] L. Kim and C. H. Green, *J. Phys. B* **22**, L175 (1989).
- [14] S. H. Vosko, J. B. Lagowski, and I. L. Mayer, *Phys. Rev. A* **39**, 446 (1989).
- [15] W. R. Johnson, J. Sapirstein, and S. A. Blundell, *J. Phys. B* **22**, 2341 (1989).
- [16] P. Krylstedt, N. Elander and E. Brändas, *J. Phys. B* **22**, 1623 (1989).
- [17] C. W. Bauschlicher Jr., S. R. Langhoff and P. R. Taylor, *Chem. Phys. Lett.* **158**, 245 (1989).
- [18] G. F. Gribakin, B. V. Gul'tsev, V. K. Ivanov and M. Yu Kuchiev, *J. Phys. B* **23**, 4505 (1990).
- [19] A. A. Gribakina, G. F. Gribakin, and V. K. Ivanov, *Phys. Lett. A* **168**, 280 (1992).
- [20] P. Fuentealba, A. Savin, H. Stoll, and H. Preuss, *Phys. Rev. A* **41**, 1238 (1990).
- [21] R. D. Cowan and M. Wilson, *Phys. Scr.* **43**, 244 (1991).
- [22] V. A. Dzuba, V. V. Flambaum, G. F. Gribakin, D. P. Sushkov, *Phys. Rev. A* **44**, 2823 (1991).
- [23] S. H. Vosko, J. A. Chevary and I. L. Mayer, *J. Phys. B* **24**, L225 (1991).
- [24] H. W. van der Hart, C. Laughlin, and J. E. Hansen, *Phys. Rev. Lett.* **71**, 1506 (1993).
- [25] D. Sundholm and J. Olsen, *Chem. Phys. Lett.* **217**, 451 (1994).
- [26] W. P. Wijesundera, S. H. Vosko and F. A. Parpia, *J. Phys. B* **29**, 379 (1996).
- [27] S. Salomonson, H. Warston, and I. Lindgren, *Phys. Rev. Letters* **76**, 3092 (1996).
- [28] I. Lindgren, *J. Phys. B* **7**, 2441 (1974).
- [29] I. Lindgren and J. Morrison, *Atomic Many-Body Theory*, (Springer-Verlag, Berlin, 1985), 2nd ed.

- [30] S. A. Blundell, W. R. Johnson, Z. W. Liu, and J Sapirstein, Phys. Rev. A **40**, 2233 (1989).
- [31] S. A. Blundell, W. R. Johnson, and J. Sapirstein, Phys. Rev. A **38**, 4961 (1988).
- [32] W. R. Johnson, M. Idrees, and J. Sapirstein, Phys. Rev. A **35**, 3218 (1987).
- [33] V. Kvasnička, Adv. Chem. Phys. **36**, 345 (1977).
- [34] I. Lindgren, J. Phys. B **24**, 1143 (1991).
- [35] J. Sucher, Phys. Rev. A **22**, 348 (1980).
- [36] W. R. Johnson, D. S. Guo, M. Idrees, and J. Sapirstein, Phys. Rev. A **34**, 1043 (1986).
- [37] E. Avgoustoglou, W. R. Johnson, Z. W. Liu, and J. Sapirstein, Phys. Rev. A **51**, 1196 (1995).
- [38] E. Avgoustoglou and Z. W. Liu, Phys. Rev. A **54**, 1351 (1996).
- [39] J. J. Novoa, F. Mota, and A. C. Ramirez, Theor. Chim. Acta **72**, 325 (1987).
- [40] H. Nakano and S. Obara, Theor. Chim. Acta **86**, 369 (1993).
- [41] W. R. Johnson, S. A Blundell, and J. Sapirstein, Phys. Rev. A **37**, 307 (1988).
- [42] B. Huron, J. P. Malrieu, and P. Rancurel, J. Chem. Phys. **58**, 5745 (1973).
- [43] A. E. Litherland, L. R. Kilius, M. A. Garwan, M.-J. Nadeau, and X.-L. Zhao, J. Phys. B **24**, L233 (1991)

# FIGURES

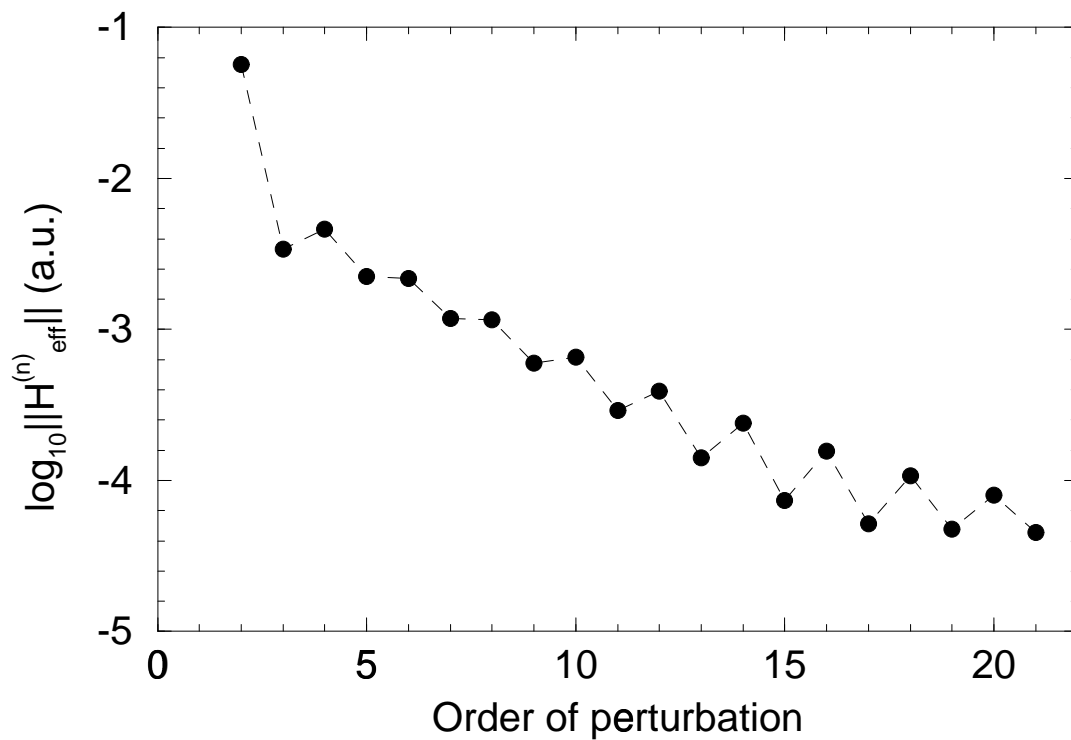


FIG. 1. The logarithm of ten of the norm of the  $n$ th-order contribution ( $H_{\text{eff}}^{(n)}$ ) to the effective Hamiltonian, in atomic units, for the  $4p_{1/2}$  state of  $\text{Ca}^-$ .

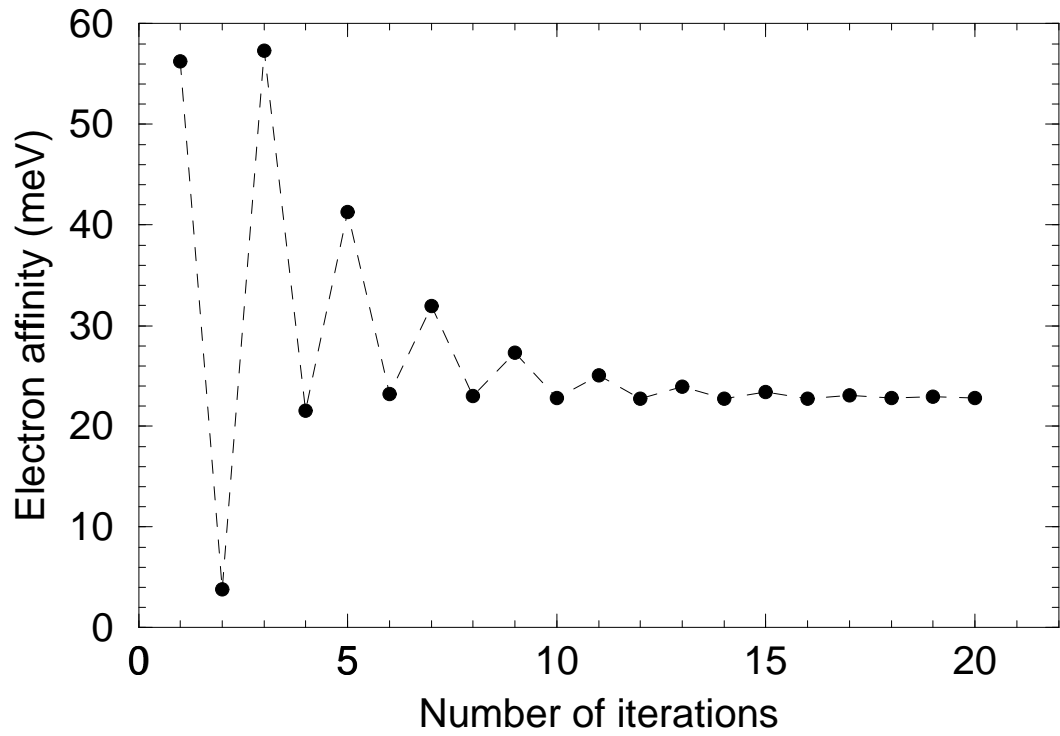


FIG. 2. The convergence pattern for the electron affinity of the  $4p_{1/2}$  state of  $\text{Ca}^-$  derived from the diagonalization of the iterated  $H^{\text{eff}}$ .

TABLES

TABLE I. Calculated electron affinities from second-order Dyson eq.  $E_{\text{Dyson}}^{(2)}$ , second-order  $H^{\text{eff}} E^{(2)}$  and all-orders  $H^{\text{eff}} E^{(\text{pair})}$  along with the lowest-order Breit  $B^{(1)}$  for  $\text{Ca}^-$ ,  $\text{Sr}^-$ ,  $\text{Ba}^-$  and  $\text{Yb}^-$  in comparison with most recent experiments.  $E^{(\text{tot})} = E^{(\text{pair})} + B^{(1)}$ . Active core is given in parenthesis. Units: meV

State	$E_{\text{Dyson}}^{(2)}$	$E^{(2)}$	$E^{(\text{pair})}$	$B^{(1)}$	$E^{(\text{tot})}$	Exp.
$\text{Ca}^-(3s^2 3p^6 4s^2)$						
$4p_{1/2}$	57.8	56.2	22.8	-0.4	22.4	24.55(10) <sup>a</sup>
$4p_{3/2}$	51.4	50.2	18.4	-0.3	18.1	19.73(10) <sup>a</sup>
$\text{Sr}^-(3d^{10} 4s^2 4p^6 5s^2)$						
$5p_{1/2}$	101.7	98.8	48.8	-0.9	47.9	48(6) <sup>b</sup>
$5p_{3/2}$	77.1	74.2	37.4	-0.6	36.8	
$\text{Ba}^-(4d^{10} 5s^2 5p^6 6s^2)$						
$6p_{1/2}$	204.7	200.6	147.0	-1.7	145.3	144.62(6) <sup>c</sup>
$6p_{3/2}$	141.3	136.6	97.3	-1.1	96.2	89.60(6) <sup>c</sup>
$\text{Yb}^-(4d^{10} 5s^2 5p^6 4f^{14} 6s^2)$						
$6p_{1/2}$	45.0	48.4	$\approx 0$			$> 10^d$

- a.* Ref. [7].
- b.* Ref. [8].
- c.* Ref. [9].
- d.* Ref. [43].

TABLE II. Comparison of the electron affinities and the corresponding fine-structure splittings  $\Delta E_{fs}$  for  $\text{Ca}^-$ ,  $\text{Sr}^-$  and  $\text{Ba}^-$  with other many-body calculations. Units: meV

	$\text{Ca}^-$			$\text{Sr}^-$			$\text{Ba}^-$		
	$4p_{1/2}$	$4p_{3/2}$	$\Delta E_{fs}$	$5p_{1/2}$	$5p_{3/2}$	$\Delta E_{fs}$	$6p_{1/2}$	$6p_{3/2}$	$\Delta E_{fs}$
This Work	22	18	4.3	48	37	11.1	145	96	49.1
Salomonson <i>et al</i> <sup>a</sup>	19	13	6.2	54	29	25			
Johnson <i>et al</i> <sup>b</sup>	57			93			192		
Dzuba <i>et al</i> <sup>c</sup>	56	49	6.9	102	80	22			57
Gribakin <i>et al</i> <sup>d</sup>	58			129			144		
Experiment	24.55(10) <sup>e</sup>	19.73(10) <sup>e</sup>	4.8 <sup>e</sup>	48(6) <sup>f</sup>		26(8) <sup>f</sup>	144.62(6) <sup>g</sup>	89.60(6) <sup>g</sup>	55.02(9) <sup>g</sup>

*a.* Ref. [27].

*b.* Ref. [15].

*c.* Ref. [22].

*d.* Ref. [18].

*e.* Ref. [7].

*f.* Ref. [8].

*g.* Ref. [9].